Extended Abstracts of the 1996 International Conference on Solid State Devices and Materials, Yokohama, 1996, pp. 571-573

Missing-Dimer Structures and Their Kink Defects on MBE-Grown (2x4) Reconstructed (001)InP Surfaces Studied by UHV Scanning Tunneling Microscope

Yasuhiko ISHIKAWA, Takashi FUKUI and Hideki HASEGAWA

Research Center for Interface Quantum Electronics and Graduate School of Electronics and Information Engineering, Hokkaido University, N13 W8, Sapporo, 060 Japan

InP(001)-(2x4) reconstructed surface prepared by gas source molecular beam epitaxy (GSMBE) was studied by ultrahigh-vacuum scanning tunneling microscopy (UHV-STM) in combination with X-ray photoelectron spectroscopy (XPS) measurement. It was found that the missing-dimer structures and their kink defects on InP have remarkably different properties from those of GaAs. Based on the observation, a new missing-dimer structure is proposed for InP (2x4) surface. No correlation was found on InP between kink defects and Si doping, although the XPS peaks showed clear existence of Fermi level pinning.

1. Introduction

The ultrahigh-vacuum scanning tunneling microscope (UHV-STM) is a powerful tool for investigating the atomic arrangements on solid state material surfaces. The recent UHV-STM studies on (2x4) (and/or c(2x8)) reconstructed GaAs (001) surfaces have clarified details of the missing-dimer structures.[1-4] In particular, Pashley *et al.*[2] have found that the so-called kink defects in the missing-dimer arrangements have close correlation with Si doping, and proposed that kink defects act as surface acceptors and cause Fermi level pinning on molecular beam epitaxy (MBE) grown n-type GaAs clean (2x4) surfaces. However, no such detailed study has been made on (2x4) reconstructed InP (001) surfaces.

The purpose of this paper is to study the missing-dimer structures on (2x4) reconstructed (001) InP surfaces in detail by UHV-STM in combination with X-ray photoelectron spectroscopy (XPS) measurement.

It was found that the unit cell of the InP(001)-(2x4) surface possesses two dimers and two missing-dimer rows, as in the case of GaAs(001)-(2x4), but, in the second layer, In atoms are present in the missing-dimer trenches whereas no Ga is present in the missing-dimer trenches on GaAs as reported recently.[4]

As to the kink defects, InP has long and straight extensions of linear arrays of dimers with lower densities of kinks than those of GaAs. No correlation was found on InP between kink defects and Si doping, although XPS peaks showed clear existence of Fermi level pinning.

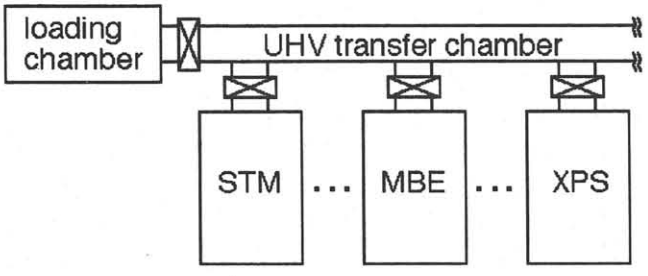

Fig. 1 UHV-based multi-chamber system used in this study.

2. Experimental

A UHV-based multi-chamber system shown in Fig. 1 was used where gas source (GS) MBE, XPS (Perkin-Elmer PHI 5100C) and UHV-STM (JEOL JSTM-4600) are connected by a UHV transfer chamber. N-type (2x4) surfaces were prepared on Si doped n-type InP epitaxial layers grown by GSMBE on (001) InP substrates using tertiarybutylphosphine (TBP), metallic In and elemental Si at 470℃. On the other hand, p-type InP (2x4) surface was prepared on a Zn doped p-type substrate by thermal desorption of surface oxides in a phosphorus flux at 500℃.

Reconstruction patterns were monitored by reflection high-energy electron diffraction (RHEED) with an electron energy of 15 keV. RHEED patterns were streaky (2x4) with long persistent RHEED oscillations during the growth. After the growth, the sample was annealed at growth temperature for 3 min in a phosphorus flux.

The (2x4) reconstructed surface obtained under P-stabilized condition at high temperatures could not maintained but changed to P-excess (2x1) reconstruction, when the surface was cooled in the chamber below 400℃.[5,6] The (2x4) surface was then recovered at room temperature by annealing the (2x1) surface at 380℃ in the MBE chamber after residual P was sufficiently removed.[6] For comparison, conventional solid source MBE-grown GaAs (2x4) surfaces were also prepared. After the (2x4) RHEED pattern was confirmed at room temperature, the sample was transferred for STM and XPS measurements through the UHV transfer chamber.

STM observations were carried out at room temperature with a constant current mode (0.10nA) at sample bias of -2.0 V (i.e. filled state images). XPS measurements were also done using a Mg$K\alpha$ radiation ($h\nu$ = 1253.6 eV) for investigating the surface Fermi level position.

3. Experimental Results and Discussion

3.1 *Missing-dimer structures on InP*

The STM images of (2x4) reconstructed InP and GaAs surfaces are shown in Figs. 2(a) and 2(b), respectively.

Figures 2(c) and 2(d) are the line-scan profiles along <110> direction including one monolayer (ML) step for each materials. Periodic dark and bright lines along <$\bar{1}$10> direction were observed on InP with the periods of 1.7 nm in <110> direction and 0.8 nm in <$\bar{1}$10> direction, indicating presence of (2x4) unit cells. For GaAs, individual dimers could be clearly resolved, and the (2x4) unit cell included two dimers and two missing-dimer rows as reported recently.[2-4]

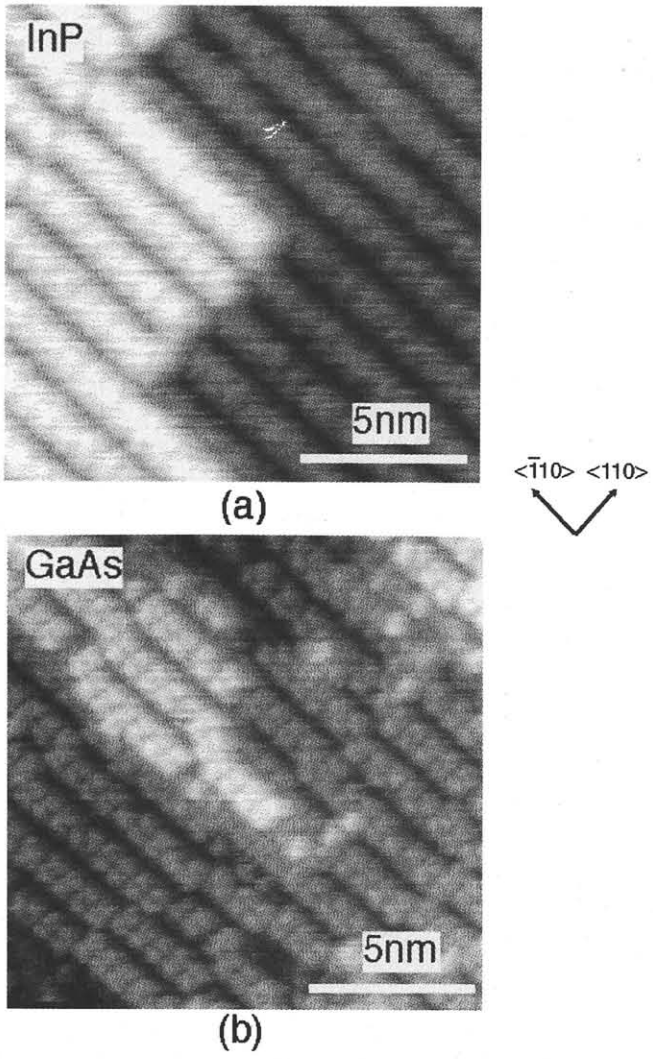

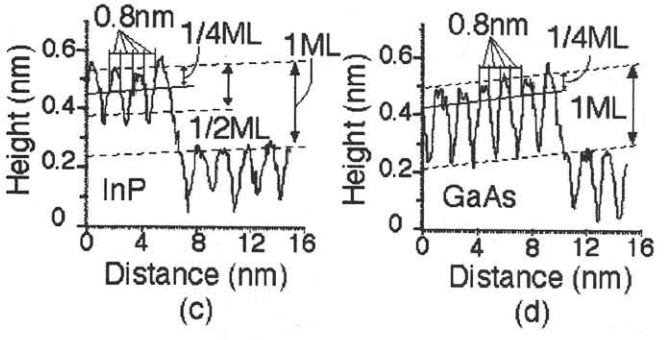

Fig. 2. STM images of (a) InP and (b) GaAs (2x4) surfaces, and the <110> line-scans of (c) InP and (d) GaAs.

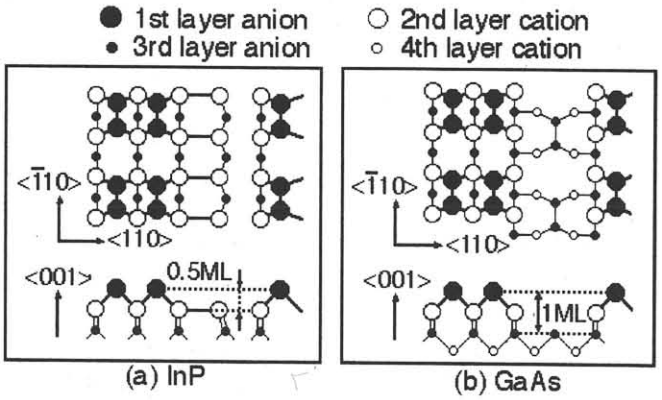

Fig. 3. A new model for InP(001)-(2x4) structure in comparison with recent model for GaAs(001)-(2x4) structure.

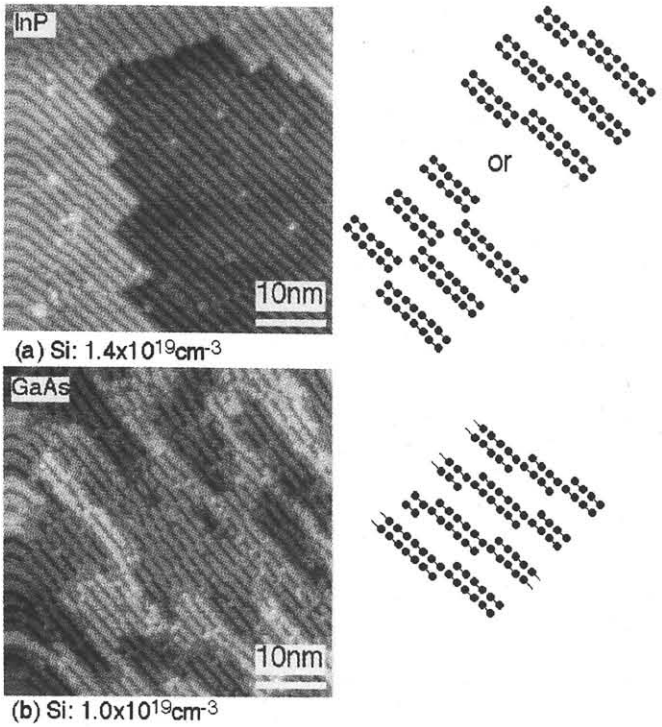

Fig. 4. STM images (50 nm x 50 nm) of (a) InP and (b) GaAs (2x4) surfaces. Right side diagrams show the schematic arrangements of the dimers.

For InP, the sine-like line-scan in Fig. 2(c) had the same width (0.8 nm) for dimer and missing-dimer parts on the center line (0.25 ML depth), showing that the InP (2x4) unit cell has also two dimers and two missing-dimer rows. However, remarkable difference exists. Namely, the amplitude of the line-scan curve of InP shown in Fig. 2(c) was equal to 0.5 ML height, but that of GaAs shown in Fig. 2(d) was equal to 1 ML height. This difference is deduced to come from the fact whether the second layer cation atoms are present or absent in the missing-dimer trenches. From this, a new model for the atomic arrangement of InP(001)-(2x4) surface shown in Fig. 3(a) is proposed here, which is different from the recent model for GaAs[4] shown in Fig. 3(b).

3.2 *Kink defects and Fermi level pinning*

As seen in Fig. 4, kinks in missing-dimer rows were observed for both highly Si-doped InP (Si:1.4x10^{19} cm^{-3}) and GaAs (Si:1.0x10^{19} cm^{-3}) (2x4) surfaces. However, the structure and the density of kinks were quite different. InP had long and straight extensions of linear arrays of dimers with lower densities of kinks than those of GaAs on which kinks appear every a few unit cells apart in the <$\bar{1}$10> direction. The right side diagrams of Fig. 4 show the schematic arrangements of the dimers. The kinks on InP are found to form the domain boundaries that run almost parallel to <110> direction.

Figure 5 shows the measured kink densities on InP and GaAs surfaces as a function of the dopant concentration. The solid lines show theoretical curves after Pashley *et al.*,[2] assuming that kinks act as surface acceptors which form dipoles with Si donors and pin the Fermi level. Although the present result on GaAs agrees with the result by Pashley *et al.*,[2] kinks on the InP surfaces show absolutely no correlation with the dopant concentration, and the density of kinks became a constant value at around 1x10^{12} cm^{-2}.

Figure 6 shows the observed peak positions of the XPS $P2p_{3/2}$ spectra of the InP (2x4) surfaces as a function of the dopant concentration. The Fermi level position was determined as shown by the solid curves in Fig. 6 after taking account of the fact that the electron escape depths (~15 Å) are comparable with the surface depletion widths for highly doped surfaces. The results clearly show the Fermi level on n-InP (2x4) surfaces is strongly pinned at around E_C-E_F = 0.4 eV. Thus, kinks that are present on the Si-doped InP surfaces can not explain the Fermi level pinning, because they had no correlation with the doping level and could not act as dominant surface acceptors. P-type STM and XPS results also show that they do not act like dominant surface donors either.

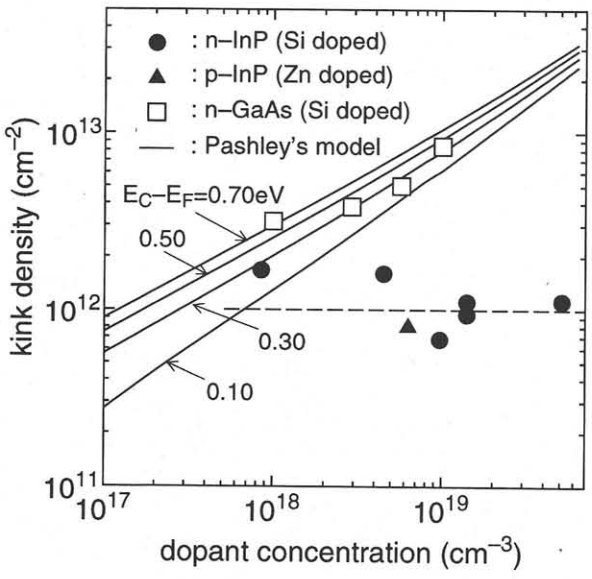

Fig. 5. Kink density vs. dopant concentration of InP and GaAs(001)-(2x4) surfaces. Solid lines show the theoretical curves after Pashley *et al.*.

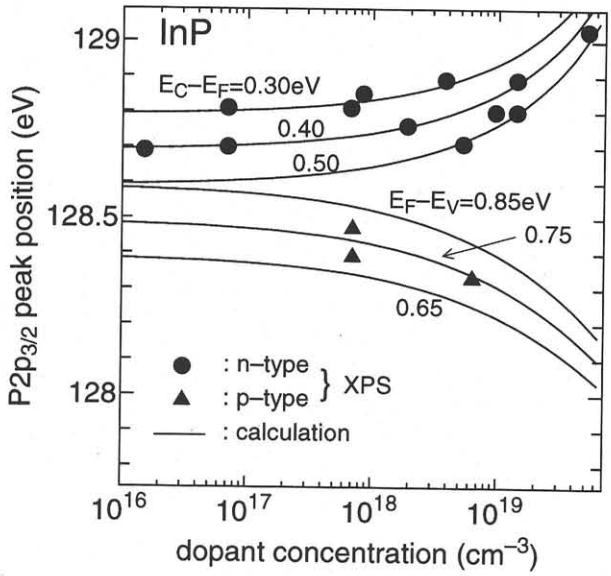

Fig. 6. XPS $P2p_{3/2}$ peak position vs. dopant concentration for InP(001)-(2x4) surfaces. Solid curves show the calculated relationship between Fermi level position and doping.

References

1) M. D. Pashley, K. W. Haberern, W. Friday, J. M. Woodall and P. D. Kirchner, Phys. Rev. Lett. **60** (1988) 2176.

2) M. D. Pashley, K. W. Haberern, R. M. Feenstra and P. D. Kirchner, Phys. Rev. **B48** (1993) 4612.

3) T. Hashizume, Q. K. Xue, J. Zhou, A. Ichimiya and T. Sakurai, Phys. Rev. Lett. **73** (1994) 2208.

4) A. R. Avery, D. M. Holmes, J. Sudijono, T. S. Jones and B. A. Joyce, Surf. Sci. **323** (1995) 91.

5) B. X. Yang and H. Hasegawa, Jpn. J. Appl. Phys. **33** (1994) 742.

6) B. X. Yang, Y. Ishikawa, T. Ozeki and H. Hasegawa, Jpn. J. Appl. Phys. **35** (1996) 1267.